FEBS Letters 588 (2014) 1637–1643

journal homepage: www.FEBSLetters.org

Detection and quantification of alternative splice sites in Arabidopsis genes AtDCL2 and AtPTB2 with highly sensitive surface enhanced Raman spectroscopy (SERS) and gold nanoprobes

Ulhas S. Kadam [a,b,c], Burkhard Schulz [b], Joseph Irudayaraj [a,c,*]

[a] Agricultural and Biological Engineering, Purdue University, West Lafayette, IN 47907, United States
[b] Horticulture and Landscape Architecture, Purdue University, West Lafayette, IN 47907, United States
[c] Bindley Bioscience Center at Discovery Park, West Lafayette, IN 47907, United States

ARTICLE INFO

Article history:
Received 31 January 2014
Accepted 28 February 2014
Available online 12 March 2014

Edited by Michael R. Sussman

Keywords:
Raman spectroscopy
Alternative splicing
Gold-nanoprobe
mRNA
Arabidopsis thaliana

ABSTRACT

Alternative splicing (AS) increases the size of the transcriptome and proteome to enhance the physiological capacity of cells. We demonstrate surface enhanced Raman spectroscopy (SERS) in combination with a DNA hybridization analytical platform to identify and quantify AS genes in plants. AS in AtDCL2 and AtPTB2 were investigated using non-fluorescent Raman probes using a 'sandwich assay'. Utilizing Raman probes conjugated to gold nanoparticles we demonstrate the recognition of RNA sequences specific to AtDCL2 and AtPTB2 splice junction variants with detection sensitivity of up to 0.1 fM.

1. Introduction

Alternative splicing (AS) is a process which generates different mature mRNAs from a single pre-mRNA by varying splice sites. AS expands the information content of eukaryotic genomes and can affect the stability and translation efficiency of mRNA [1,2]. AS has been implicated in diseases such as cancer [3]. In mammals, a number of genes undergo AS, which results in the expansion of the protein repertoire encoded by the respective genome. This process creates novel functions by affecting the structure of proteins. Additionally, interaction with different protein partners due to the rearrangement of interactive surfaces can be modified by AS [4]. AS has been well studied in model animals as a post-transcriptional gene regulation strategy to increase transcriptome and the proteome variability for added physiological function [5], but its role in plants is less understood.

AS analysis in plants has been documented on only a few occasions [2,6–9], even though the first discovery of AS was reported 25 years ago in a rubisco activase gene [6]. Until now, most reports have mapped AS in plant genes but have rarely explored it in a quantitative manner. The significance of AS in plants has been a matter of debate and the number of genes subjected to AS were considered negligible by many researchers. Global gene expression studies using RNA-seq and the availability of transcriptome sequence databases showed that AS in plants is highly significant [10,11]. Interestingly, reports on AS in plants have increased over the last few years due to improved RNA analysis technology. From 2003 [12] until 2012 [13], new technologies increased the detection of AS from 1.2% to 61% of all genes of the Arabidopsis genome. The quantification of AS has improved due to read counts in RNA-seq experiments, but still depends on the depth of sequencing and the efficiency of cDNA synthesis and sequencing [14].

The availability of EST databases has enabled scientists to identify AS through alignments of ESTs to reference genomes [1,15]. This procedure has been used for the generation of AS databases for many mammals [16]. However, Expressed Sequence Tags (EST) sequencing is often biased toward the 3′ and 5′ ends of mRNA transcripts. Further, there is limited coverage of ESTs or cDNAs of sequenced transcripts from certain cell or tissue types or under defined environmental conditions to infer occurrence of AS [4]. Some limitations inherent in the analysis of EST/cDNA have been

* Corresponding author at: Department of Agricultural and Biological Engineering, Purdue University, 225 South University Street, ABE 215, West Lafayette, IN 47907, United States. Fax: +1 765 496 1115.
E-mail address: josephi@purdue.edu (J. Irudayaraj).

http://dx.doi.org/10.1016/j.febslet.2014.02.061
0014-5793/Published by Elsevier B.V. on behalf of the Federation of European Biochemical Societies.

overcome by the development of custom microarrays as well as by differential hybridization techniques, which permit large-scale profiling of AS [4,5,17]. AS microarrays are often based on sets of anchored oligonucleotide probes, which typically combine probes specific to individual exons and/or splice-junction sequences formed by inclusion or skipping of exons and retention of introns. This format permitted the discovery of new AS events not previously detected [17]. However, this approach cannot be applied for gene specific analysis of AS events in a quantitative manner as the sensitivity of microarray hybridization is very limited due to the dependence on the fluorescence signal and the detection modality. Quantification of bound molecules is therefore only possible for a limited range of detection. In addition, the distinction of different hybridized AS variant RNA molecules is sometimes not possible as different AS variants contain identical sequence stretches that overlap.

To address these challenges, a SERS-based mRNA monitoring strategy holds promise because of its flexibility in multiplexing and potential for highly sensitive detection of rare RNAs [18]. The use of chemically characterized, non-fluorescent Raman probes makes accurate quantification of AS transcripts possible [19]. Raman nanoprobes can be designed for quantification due to their high reproducibility and homogeneous surface enhancement. With current methods, nearly uniform enhancement is possible and is a significant step in SERS-based quantification. Further, SERS-based quantification has the potential to be more sensitive than fluorescence based assays [20–22].

Here, we integrate principles of nanotechnology, Raman spectroscopy and genetics to develop a highly sensitive RNA detection system for plants. The evidence for AS's biological significance is becoming stronger as more cases of AS are being reported in plants [2]. Conventional methods to assess and quantify AS rely on technology that is less sensitive, such as RNA hybridization based on fluorescent readouts, or methods with cumulative error during amplification steps via PCR, such as RNA-seq. We consider the hybridization step-based detection and quantification, which does not rely on enzymatic activities during amplification and sequencing processes found in many RNA-seq approaches, an advantage in terms of reliability of the method. Even new developments such as Single Molecule Real-Time DNA Sequencing (SMRT DNA Sequencing) found in the next generation sequencing methods from Pacific Biosciences utilize (PacBio RS) immobilized DNA polymerases. SERS-based detection and quantification of AS and rare mRNAs will significantly enhance research in plant gene regulation. Quantification and testing of AS in plants in a multiplex format will also allow process automation to help address unanswered questions in plant biology. SERS-based AS analysis is a promising method because of multiplexing capability, high specificity, and sensitivity. Single SERS experiments allow targeted approaches, with ability to probe a smaller number of genes and do not require a genome-wide approach, which often produces a vast amount of data, which needs extensive analysis and an expert team of bioinformaticians. The proposed method was developed using well-characterized SERS-substrates and non-fluorescent Raman probes with unique and narrow spectral peaks. The narrow spectral widths are useful to reduce the cross-talk among Raman probes, could resolve spectral interactions to within 10 nm and hence could be exploited for multiplex detection unlike fluorescent probes, whose peaks are very broad. Recent progress in nanomaterials for SERS substrate synthesis using gold nanoparticles (AuNPs) and nano-conjugation strategies have made a highly uniform and reproducible enhancement possible. SERS-based detection of DNA or RNA has been shown to be highly specific and sensitive compared to fluorescence assays [21,23].

This innovative approach of SERS-based array format could capitalize on the availability of numerous non-fluorescent probes with distinct Raman spectra and the assay can be performed at a fraction of the cost of fluorescence assays. The Raman fingerprint is capable of identifying each non-fluorescent label at a resolution of 10 nm, whereas bandwidth of fluorescence spectra is 100–300 nm and that of quantum dots is 40–50 nm [24]. Quantification at femto-molar concentration and single molecule sensitivity enables the detection of rare splice variants, which otherwise go undetected in traditional approaches.

We investigated AS in two genes, AtDCL2 and AtPTB2, which are highly significant in plant developmental and RNA biology. DICER-LIKE (DCL) genes are dedicated to function in small RNA regulation via RNA interference [25]. DCL2 is a regulator of siRNAs and has a key role in plant egg cell development. It guides mRNAs to nuclease digestion or translational inhibition. AtDCL2 acts as the trigger for siRNA biogenesis or RNAi pathways in the egg cell and is required for egg cell maturation, fertilization, and embryogenesis [26].

Polypyrimidine tract-binding protein (PTB) was identified as a nuclear-localized splicing factor that specifically binds to polypyrimidine tracts within pre-mRNA introns [27]. AtPTB2 influences splice site selection and coordination of splicing events. We analyzed AS of AtPTB2 and provide evidence of its auto-regulation of AS [28]. Arabidopsis PTB homologues are subject to extensive auto- and cross-regulation via AS-coupled nonsense mediated decay, thereby establishing their significance in gene expression by regulating AS events [29,30]. PTB represents a regulatory link between RNAs and a variety of cellular factors in both, the nucleus and cytoplasm. PTB is critical for growth, development, and reproduction including pollen germination. It functions as regulator of cell differentiation and development [31]. PTB is involved in RNA metabolism and is the most studied regulator of AS. Additionally, PTBs appear to function as RNA chaperons, resulting in the attainment of the correct functional conformation of IRES (internal ribosome entry segment) [31,32]. PTB functions in site-specific intracellular localization and sorting of mRNA and in controlling the stability of mRNA via binding to pyrimidine tract binding sites within 5′- and 3′-untranslated regions [33].

2. Materials and methods

2.1. Chemicals

DNA oligonucleotides obtained from IDT-DNA (Coralville, IA). Gold(lll)-chloride trihydrate, tris(2-carboxyethyl)phosphine hydrochloride (TCEP), Tween-20, trisodium citrate dehydrate, Na-EDTA were obtained from Sigma–Aldrich (St. Louis, MO). Other chemicals used in this study were obtained from Purdue University stores.

2.2. Hybridization of mRNA to ssDNA targets

Total RNA was extracted from 100 mg of leaf tissue from 4 to 5 week old plants grown under greenhouse conditions. The quality of extracted RNA was tested using 2% Agarose gel electrophoresis [34,35]. RNA quality was validated using the Agilent 2100 Bioanalyzer (Agilent Technologies, Inc.). The total RNA was quantified and checked for quality with a NanoDrop 2000c photometer (Thermo Scientific, Wilmington, DE). To remove any DNA contaminations the DNA-Free RNA Kit (R1013) from Zymo Research, Irvine, CA was used. Total RNA was incubated for 30 min at 37 °C with DNase I component of the kit and cleaned up after incubation with Zymo-Spin IC columns according to the provided protocol. Successful removal of DNA contaminations was tested using intron-specific primers via RT-PCR. A hybridization cocktail of 30 μL was prepared as follows: (20 μL of DNase-treated total-RNA, 9 μL of a 3×

hybridization solution: 3 M NaCl, 0.5 M HEPES, 1 mM EDTA; and 1 μL (0.3 ng) of DNA oligonucleotides (target strand) with sequences complementary to the mRNA transcripts. This mixture was heated at 75 °C for 10 min and incubated overnight at 55 °C to form RNA–DNA hybrid. 270 μL of S1 nuclease mix (S1 nuclease mix (300 μL): 30 μL of 10× S1 nuclease buffer, 0.25 μL of S1 nuclease (Invitrogen, Carlsbad, CA), 0.6 μL of 10 mg/mL calf thymus DNA (R&D Systems, Minneapolis, MN). Fifteen μL RNase-free water was added, and incubated at 37 °C for 45 min. Then 50.6 μL of hydrolysis solution (1.6 M NaOH and 135 mM EDTA) was added to digest the RNA copy from the RNA–DNA hybrids and the mixture was incubated at 95 °C for 15 min. Finally, the reaction mix was neutralized with 50.6 μL neutralizing solution (1 M HEPES, 1.6 M HCl, and 6× SSC) to stabilize the DNA targets at neutral pH [36,37].

2.3. Reverse transcription and PCR amplification of AS variants

Reverse transcription and PCR was performed as described in [38].

2.4. Characterization of nanoparticles

UV–Vis spectra were recorded with a V-570, Rev. 1.00 spectrometer (JASCO Inc., Easton, MD). Transmission electron micrographs (TEM) were taken using a Philips CM-100 TEM (FEI-Company, Hillsboro, OR) operated at 100 kV, spot-3, 200 μm condenser aperture and 70 μm objective aperture. Images were captured with a SIA-L3-C digital camera coupled with high-magnification electron microscope. Nanoparticle samples of 4 μL (0.3 nM) were spotted on a 400 × 400 mesh grid with formvar + carbon film and glow discharged prior to use. A 2%-uranyl acetate (UA) stain was used to negatively stain the samples. The grid was floated on sample droplets for ~1 min exposure prior to rinsing in staining solution droplets and dried by blotting. Zeta potential was measured using Zetasizer Nano (Malvern Instruments, Worcestershire, UK) [38]. Each sample size was measured at least three times.

2.5. Synthesis of DNA–AuNP-RTag probes

Thiolated DNA oligos were reduced using a 10 M solution of TCEP (RT, shaking for 15 min). The reduced thiolated probing DNA strands (1 μM) were then added to the precipitate obtained from 10 ml of AuNPs solution to obtain a 1 ml solution and then, incubated at room temperature for 24 h (on shaker). Next, the solution was buffered at pH 7.4 using 10 mM phosphate buffer and 0.01% Tween-20 and salted slowly with 4 M NaCl to reach a final salt concentration of 0.3 M. After 'aging' for 40 h (shaking at RT) and washing, 1 ml of Raman tag solution 4-mercaptobenzoic acid was added and incubated for 24 h (shaking at RT). The resulting DNA–AuNP-Raman tag probes were washed three times with 0.3 M *P*hosphate *B*uffered *S*aline (PBS, pH 7.5) to remove excess Raman tags [37,38].

2.6. SERS sandwich assay

For the SERS sandwich assay, gold-coated glass slides were first treated with piranha solution (3:1::H_2O_2:H_2S_4) for 1 h. Subsequently the slides were covered with a silicone mask with an array of holes (3 mm diameter) to avoid cross contamination. 10 μL of 1 μM CS with 3′-thiol modification was spotted onto the slide and incubated in a humidity chamber at RT for 6 h. Then, 10 μL of 1.0 mM 6-mercapto-1-hexanol was added and incubated overnight in a humidity chamber at RT to avoid non-specific binding. Next, 10 μL of the target strand was added to hybridize with the immobilized CS by incubating in a humidity chamber at 37 °C for 4 h. Finally, 10 μL of a DNA–AuNP-RTag probe was added, which is functionalized with PS with 5′-thiol modification and non-fluorescent Raman tags covalently attached to 30 nm gold nanoparticles. This sandwich structure was incubated in a humidity chamber (37 °C, 4 h) and then washed three times with 1× PBS to remove unbound probe strands [37]. Finally, the gold slides with immobilized oligos were analyzed using Raman spectroscopy (Senterra, Bruker Optics, Ewing, NJ). The sandwich structure with Raman probes was excited using the 765 nm laser at 10 mW power at the source. For determination of absolute quantities of AS variants, a calibration was developed based on a known molar concentration of target strands and plotted against the normalized Raman intensity (concentration vs intensity) peak of 1075 cm^{-1} to obtain a standard equation.

Table 2
PCR primers for the detection of AS AtDCL2 and AtPTB2 mRNAs.

DCL2_F_Exon3_Intron_2	5′-CTTGTCACTCAGGTATTGGT-3′
DCL2_R_Exon4_Intron_2	5′-CTTCTGCTTGCTGCGTAAAACA-3′
PTB_2_F_Exon_2	5′-GCTTCTTCTTCGGAGCCTGCT-3′
PTB_2_R_Exon_4	5′-AGGGATGCTTCTTCCATCGAG-3′

3. Results and discussion

For the detection of AS by SERS, AtDCL2 and AtPTB2 were selected. The selection was based on bioinformatics analysis of AS in Arabidopsis using the TAIR-10 database [39]. AS targets AtDCL2 and AtPTB2 are important for plant development and RNA dynamics. After selection of AS genes, the probes (target strand, probing strand, capture stands, Table 1) and PCR primers (Table 2) were designed for the investigated splice junctions (Fig. 1). For AtDCL2 (AT3G03300) splicing variants AT3G03300.1 and AT3G03300.3 are predicted using bioinformatics. In the case of AtPTB2 (AT5G 53180) the two splicing variants AT5G53180.1 and AT5G53180.2 were predicted. In this study we selected one AS variant to quantify the AS transcript for each gene as proof-of-concept study. For the analysis of gene expression, plants were grown under greenhouse conditions as described in Section 2. Mature leaf tissues were used for RNA extraction. The total RNA extraction was performed using the acidic phenol (pH~4.7) method with few modifications for Arabidopsis leaf tissue [34,35]. Samples with a spectral 260/280 nm ratio of 2.0–2.2 and an RNA integrity number (RIN) above >7.5 were chosen for Raman and qRT-PCR analysis.

Well-characterized SERS substrates were used in this study for uniform signal enhancement and reproducibility. The morphology and structure of the naked and the conjugated nanoparticles were determined using TEM, UV–Vis and Zetasizer as described in Section 2. The TEM imaging confirmed that the synthesized gold

Table 1
Oligonucleotide probes for SERS-based analysis of AS of AtDCL2 and AtPTB2 gene splice junctions.

DCL2_Ex2_3′_Intron2_5′_TS	5′-AAGTGGTTCTTGTCACTCAGGTATTGGTGTTAGGATTGGA-3′
DCL2_CS_Exon_2	5′-CTGAGTGACAAGAACCACTTttttttttt/3ThioMC3-D/-3′
DCL2_PS_Intron_2	5′-5ThioMC6-D/ttttttttttTCCAATCCTAACACCAATAC-3′
PTB2_EX2_3′_Exon4_5′ TS	5′-GCATCGATGTTATCCATCTGGCACTAGTTCAATTTACTGA-3′
PTB2_CS_Exon_2	5′-CAGATGGATAACATCGATGCttttttttttt/3ThioMC3-D/-3′
PTB2_PS_Exon_4	5′-5ThioMC6-D/ttttttttttTCAGTAAATTGAACTAGTGC-3′

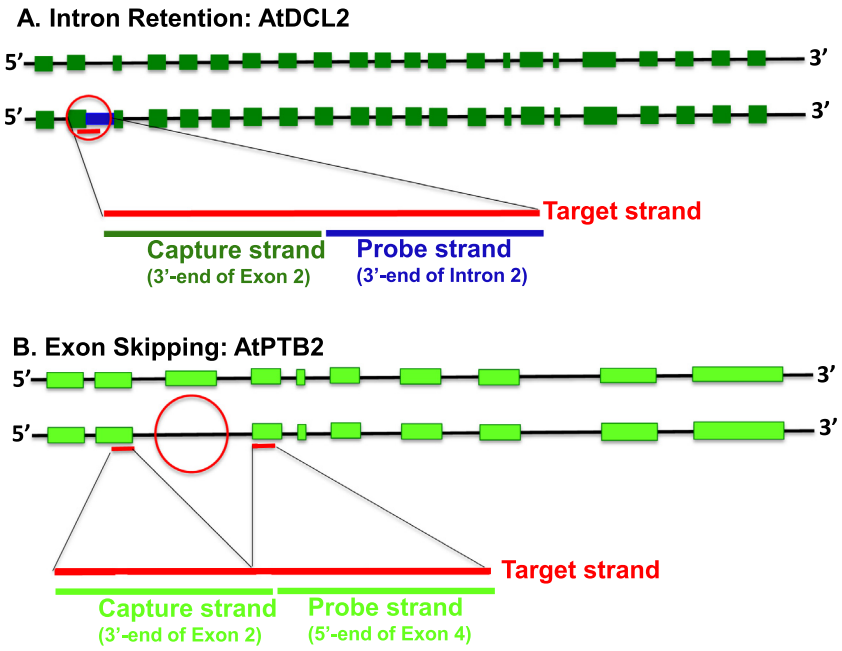

Fig. 1. Structure of alternatively spliced Arabidopsis genes AtDCL2 (A) and AtPTB2 (B). AtDCL2 shows intron retention of the second intron (blue and marked with a red circle). AtPTB2 shows exon skipping of the third exon (marked with a red circle). Exons are depicted as dark-green (AtDCL2) and light green (AtPTB2) boxes. Introns are indicated as black lines. 5′ and 3′ end of the mRNAs is indicated.

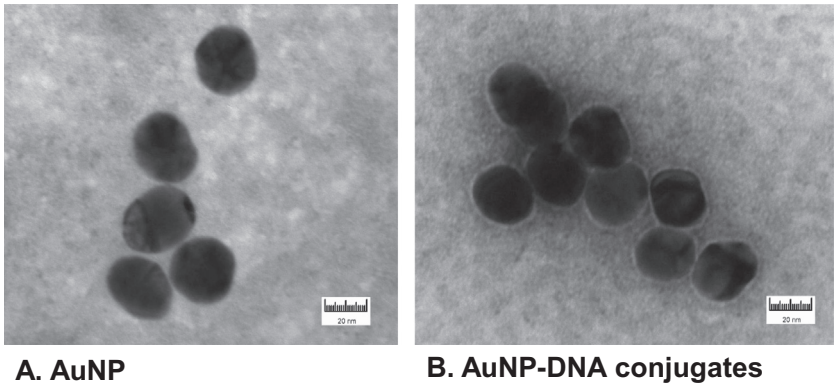

Fig. 2. TEM images of gold nanoparticles before (A) and after (B) conjugation with thiolated ssDNA oligonucleotides.

nanoparticles used were spherical in shape and the size was predominantly around 30 nm (Fig. 2). Further, 2% uranyl acetate-treated AuNPs showed a clear white layer of 1–2 nm thickness of thiolated ssDNA surrounding the particles (Fig. 2b). The UV–Vis spectra of AuNPs before (peak at 530 nm) and after conjugation with DNA (peak at 539 nm) was acquired to validate the conjugation of DNA (Fig. SI1). The UV–visible spectrum shows a 'red shift' as a function of increase in size and change in absorption. Additionally, Zeta-potential (ζ) of AuNPs was measured to confirm the covalent attachment of thiolated oligos. The stability and functionality of AuNP–DNA complex can be assessed by measuring the surface charge and ionic conditions of the surrounding microenvironment. ζ is routinely used to assess nanoparticle stability and confirm its successful conjugation. Therefore, it is important to quantify the surface charge distribution of the AuNP–DNA conjugate. For stable gold nanoparticle solution, a ζ-value of -15 to -40 is acceptable depending on the size and buffer solution. The nanoparticle solution used in this study possessed a ζ-value of -21 mV and -36.5 mV before and after ssDNA conjugation, respectively. This confirms the interaction of the conjugate with other substrates under study [40,41].

A description of the steps involved in SERS analysis of mRNA transcripts is shown in Fig. 3. The detection of mRNAs is based on three principles: (a) mechanism of DNA–RNA hybridization ('Watson-Crick' base-pairing) to capture mRNA transcripts, (b) degradation of un-hybridized ssDNA target probe and degradation of RNA molecules, and (c) biophysical basis of surface enhancement by nanoprobes (DNA–AuNP-RTag) to amplify the specific signal. A calibration curve was constructed using gold-coated glass slides, thiolated oligos, and SERS nanoprobes to construct the 'sandwich structure' with known target concentrations. The slides were covered with silicone masks to make an array of trays ($\sim$3 mm diameter) to load the samples and avoid cross contamination between samples. The thiolated capturing strand (10 nM) with sequence complementary to the downstream half of the target strand was immobilized to the well via strong 'gold-sulfur' covalent interaction [38,42]. Unbound gold slide surfaces were covered with a layer of the blocking agent 6-mercaptohexanol to avoid non-specific binding of the Raman probes [36,37,43]. Subsequently the target strands were hybridized to capturing strands through hydrogen bonding to complementary nucleotides. Finally, the probing strand comprising of DNA–AuNP-RTag conjugate was

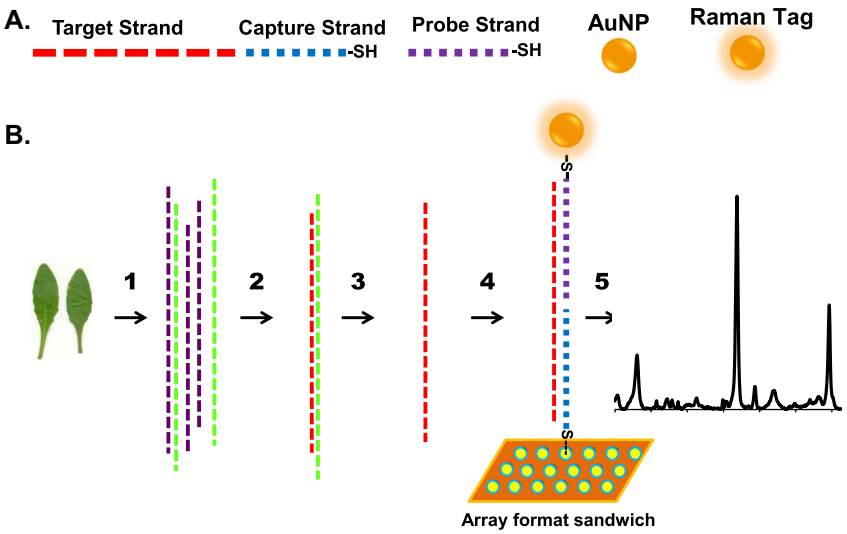

Fig. 3. Schematic representation of workflow of SERS-based quantification of AS variants in AtDCL2 and AtPTB2. (A) Substrates used in this assay: target strand, capture strand, probing strand, AuNP (gold nanoparticle), and 4-mercaptobenzoic acid (Raman probe, shown as glow around AuNPs). (B) Steps involved in constructing 'sandwich structure' and acquisition of Raman signal (1) total RNA extracted from leaves, (2) capture of target AS variants by formation RNA–DNA hybrid and digestion of the non-hybridized portion by S1 nuclease and RNA by alkaline hydrolysis, (3) representative AS variant (AtDCL2, target strand), (4) "array format sandwich structure" for SERS detection, and (5) Raman signal.

hybridized to the upstream half of the target strand to complete the sandwich structure.

A series of target strand concentrations, ranging from 10 nM to 0.10 fM was used to develop a standard curve and to determine the detection limit. 4-mercaptobenzoic acid, a non-fluorescent Raman tag was used. The Raman spectra of gold nanoprobes conjugated to 4-mercaptobenzoic acid were acquired and a Raman shift peak of 1075 cm^{-1} was chosen as a characteristic peak for further analysis (Fig. 4). After acquisition of the spectra, 'baseline correction' of each spectrum was performed using OPUS 6.0 software (Bruker Optics, Inc.). The plasmon–phonon band (180 to 230 cm^{-1}) was applied as a self-referencing internal standard [44]. The corrected characteristic peak (l_1075) (Figs. 4 and 5) was normalized against the corrected plasmon–phonon band ($l_{\sim 220}$), i.e., $|_n = l_{1075}/l_{220}$. A similar normalization process was performed with control samples without TS, the l_n obtained for controls was subtracted from the samples used in calibration. Such 'plasmon–phonon' based calibration procedure corrects for individual nanoparticle distribution and aggregation variability. At least five spectral replications were used for each analysis and separately normalized. The data points were fitted ($R^2 = 0.91$) with the signal from the MBA Raman probe at 1075 cm^{-1} (Figs. 4 and 5). The calibration method for the 'sandwich assay' compensates for all the factors, such as gold surface features, size dependency and RTag variations involved in sample preparation and detection [44].

For the qualitative validation of these results, RT-PCR was used to compare the expression of splice junctions in AtDCL2 and AtPTB2. Primers for these splice junctions were designed for specific splice junction variants. The quantification results presented in Table 3 show the detection of AS variants of AtDCL2 at 6.72 pM and AtPTB2 34.67 pM, respectively. Though sensitivity of our approach is excellent, it heavily is dependent on prior knowledge of target sequences. The quantification shows a higher expression of AtPTB2 than AtDCL2, which confirms the results from microarray hybridization expression profiles of respective genes available from the Genevestigator (For AT3G03300: 102.2 E.U. using array element 258863_AT; 248.3 E.U. using array element 258848_AT and for AT5G53180: 328.9 E.U. using array element 248304_AT) [45] and eFP Browser (73.2 E.U. for AT3G03300 and 128.4 E.U. for AT5G53180) [46] databases.

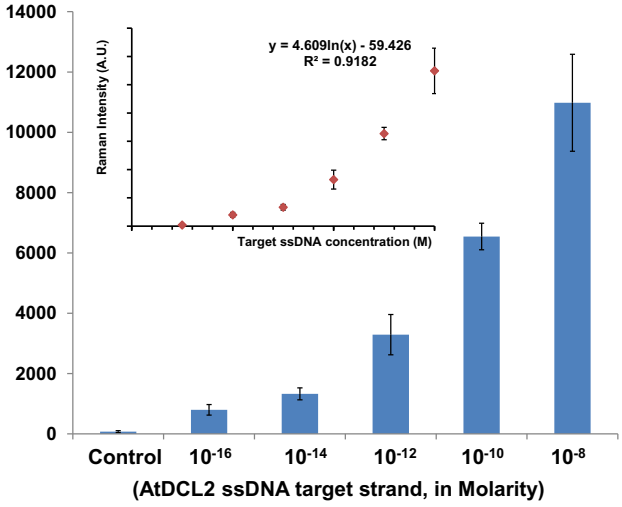

Fig. 4. The histogram shows the peak intensity at 1075 cm^{-1} (Raman shift) of control DNA ranging from 0.1 fM to 10 nM concentrations of target strands. Inset: calibration curve obtained for the quantification of target strands.

Plant developmental processes such as flowering, circadian rhythms or hormonal responses are regulated by AS [47,48]. The same can be found for responses to temperature, light and pathogens. It may be that a number of processes have not yet been identified due to the insufficient sensitivity of detection methods for rare mRNA splice variants. However, the increased number of AS genes signifies its impact in plant biology. Although the availability of EST and cDNA databases in plants has not yet reached the level of coverage for animal systems [4,49], the number of cases of AS have increased with improved sequencing technology and with more advanced data analysis tools [8–10,13,50]. Modifications of the described approach can also be used for the identification and quantification of other regulatory RNAs such small RNAs and micro-RNAs in plants at high sensitivity. Furthermore, our approach could be adopted for specific target sequences from any organism including bacteria, viruses, animals, and fungi.

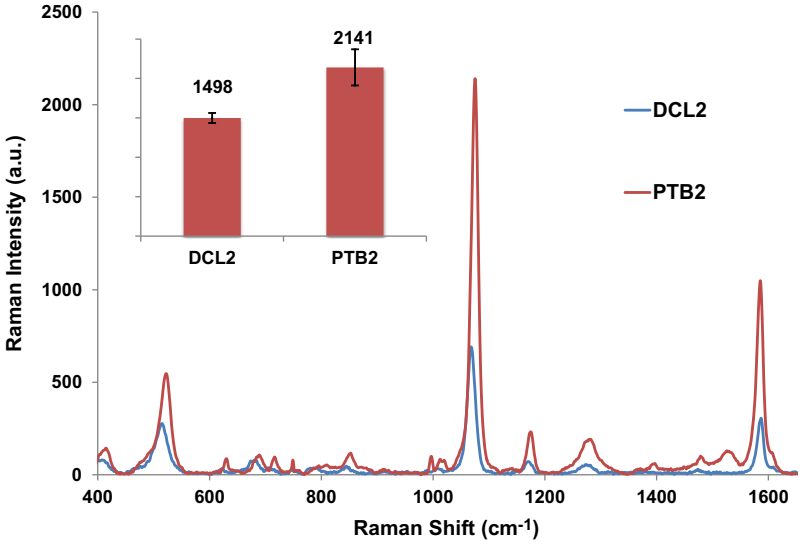

Fig. 5. Illustrative Raman spectra of AS transcripts obtained for AtDCL2 (blue) and AtPTB2 (red) from Arabidopsis leaf tissue. The inset shows a comparison of the peaks at 1075 cm^{-1}.

Table 3
Quantification of described AS variants in AtDCL2 and AtPTB2 from Arabidopsis.

AS target	Raman Intensity (AU)	Absolute concentration (pM)
AtDCL2	1498 ± 63.29	6.72
AtPTB2	2141 ± 228.7	34.87

We present the first application of SERS for mRNA detection and quantification of AS in plants (Fig. 5 and Table 3). The SERS results were validated with RT-PCR. We show the application of a novel SERS-based biophysical assay to study AS genes in plants. Such analysis will help elucidate novel functions of AS genes and the regulation of gene expression by increasing the transcriptome and proteome variability in plants. We believe that this approach could be further developed for in vivo analysis of AS isoforms at single cell resolution.

Acknowledgements

Authors gratefully acknowledge the funding from NSF-EAGER DBI-0939906 Award to B.S. and J.l. The Bilsland Dissertation Fellowship was awarded to UK from Purdue University. We thank Rosanne Altstatt for copy-editing.

Appendix A. Supplementary data

Supplementary data associated with this article can be found, in the online version, at http://dx.doi.org/10.1016/j.febslet.2014.02.061.

References

[1] Stamm, S., Riethoven, J.J., Le Texier, V., Gopalakrishnan, C., Kumanduri, V., Tang, Y., Barbosa-Morais, N.L. and Thanaraj, T.A. (2006) ASD: a bioinformatics resource on alternative splicing. Nucleic Acids Res. 34, D46–D55.
[2] Syed, N.H., Kalyna, M., Marquez, Y., Barta, A. and Brown, J.W. (2012) Alternative splicing in plants – coming of age. Trends Plant Sci. 17, 616–623.
[3] van Doom, R., Dijkman, R., Vermeer, M.H., Starink, T.M., Willemze, R. and Tensen, C.P. (2002) A novel splice variant of the Fas gene in patients with cutaneous T-cell lymphoma. Cancer Res. 62, 5389–5392.
[4] Johnson, J.M. et al. (2003) Genome-wide survey of human alternative pre-mRNA splicing with exon junction microarrays. Science 302, 2141–2144.
[5] Yeakley, J.M., Fan, J.B., Doucet, D., Luo, L., Wickham, E., Ye, Z., Chee, M.S. and Fu, X.D. (2002) Profiling alternative splicing on fiber-optic arrays. Nat. Biotechnol. 20, 353–358.
[6] Werneke, J.M., Chatfield, J.M. and Ogren, W.L. (1989) Alternative mRNA splicing generates the two ribulosebisphosphate carboxylase/oxygenase activase polypeptides in spinach and Arabidopsis. Plant Cell 1, 815–825.
[7] Kalyna, M. et al. (2012) Alternative splicing and nonsense-mediated decay modulate expression of important regulatory genes in Arabidopsis. Nucleic Acids Res. 40, 2454–2469.
[8] Ner-Gaon, H., Leviatan, N., Rubin, E. and Fluhr, R. (2007) Comparative cross-species alternative splicing in plants. Plant Physiol. 144, 1632–1641.
[9] Campbell, M.A., Haas, B.J., Hamilton, J.P., Mount, S.M. and Buell, C.R. (2006) Comprehensive analysis of alternative splicing in rice and comparative analyses with Arabidopsis. BMC Genomics 7, 327.
[10] Wang, B.B. and Brendel, V. (2006) Genomewide comparative analysis of alternative splicing in plants. Proc. Natl. Acad. Sci. USA 103, 7175–7180.
[11] Filichkin, S.A., Priest, H.D., Givan, S.A., Shen, R., Bryant, D.W., Fox, S.E., Wong, W.K. and Mockler, T.C. (2010) Genome-wide mapping of alternative splicing in *Arabidopsis thaliana*. Genome Res. 20, 45–58.
[12] Zhu, W., Schlueter, S.D. and Brendel, V. (2003) Refined annotation of the Arabidopsis genome by complete expressed sequence tag mapping. Plant Physiol. 132, 469–484.
[13] Marquez, Y., Brown, J.W., Simpson, C., Barta, A. and Kalyna, M. (2012) Transcriptome survey reveals increased complexity of the alternative splicing landscape in Arabidopsis. Genome Res. 22, 1184–1195.
[14] Bryant, D.W., Priest, H.D. and Mockler, T.C. (2012) Detection and quantification of alternative splicing variants using RNA-seq. Methods Mol. Biol. 883, 97–110.
[15] Thanaraj, T.A., Stamm, S., Clark, F., Riethoven, J.J., Le Texier, V. and Muilu, J. (2004) ASD: the alternative splicing database. Nucleic Acids Res. 32, D64–D69.
[16] Lee, C., Atanelov, L., Modrek, B. and Xing, Y. (2003) ASAP: the alternative splicing annotation project. Nucleic Acids Res. 31, 101–105.
[17] Pan, Q. et al. (2004) Revealing global regulatory features of mammalian alternative splicing using a quantitative microarray platform. Mol. Cell 16, 929–941.
[18] Kadam, U., Moeller, C.A., Irudayaraj, J. and Schulz, B. (2014) Effect of T-DNA insertions on mRNA transcript copy numbers upstream and downstream of the insertion site in *Arabidopsis thaliana* explored by surface enhanced Raman spectroscopy. Plant Biotechnol. J., http://dx.doi.org/10.1111/pbi.12161.
[19] Kneipp, H., Kneipp, J. and Kneipp, K. (2006) Surface-enhanced Raman optical activity on adenine in silver colloidal solution. Anal. Chem. 78, 1363–1366.
[20] Graham, D., Thompson, D.G., Smith, W.E. and Faulds, K. (2008) Control of enhanced Raman scattering using a DNA-based assembly process of dye-coded nanoparticles. Nat. Nanotechnol. 3, 548–551.
[21] Graham, D. and Faulds, K. (2008) Quantitative SERRS for DNA sequence analysis. Chem. Soc. Rev. 37, 1042–1051.
[22] Stokes, R.J., Macaskill, A., Lundahl, P.J., Smith, W.E., Faulds, K. and Graham, D. (2007) Quantitative enhanced Raman scattering of labeled DNA from gold and silver nanoparticles. Small 3, 1593–1601.
[23] McKeating, K.S., Dougan, J.A. and Faulds, K. (2012) Nanoparticle assembly for sensitive DNA detection using SERRS. Biochem. Soc. Trans. 40, 597–602.
[24] Kadam, U.S., Lossie, A., Schulz, B. and Irudayaraj, J. (2013) Gene expression analysis using conventional and imaging methods. in: Nucleic Acids Nanotechnology in Medicine, pp. 141-162. Springer Publications Inc., http://dx.doi.org/10.1007/978-3-642-36853-0_6, ISBN 978-3-642-36853-0.
[25] Gasciolli, V., Mallory, A.C., Bartel, DP. and Vaucheret, H. (2005) Partially redundant functions of Arabidopsis DICER-like enzymes and a role for DCL4 in producing transacting siRNAs. Curr. Biol. 15, 1494–1500.

[26] Takanashi, H., Ohnishi, T., Mogi, M., Hirata, Y. and Tsutsumi, N. (2011) DCL2 is highly expressed in the egg cell in both rice and Arabidopsis. Plant Signal. Behav. 6, 604–606.
[27] Mitchell, S.A., Spriggs, K.A., Coldwell, M.J., Jackson, R.J. and Willis, A.E. (2003) The Apaf-1 internal ribosome entry segment attains the correct structural conformation for function via interactions with PTB and unr. Mol. Cell 11, 757–771.
[28] Stauffer, E., Westermann, A., Wagner, G. and Wachter, A. (2010) Polypyrimidine tract-binding protein homologues from Arabidopsis underlie regulatory circuits based on alternative splicing and downstream control. Plant J. 64, 243–255.
[29] Ruhl, C., Stauffer, E., Kahles, A., Wagner, G., Drechsel, G., Ratsch, G. and Wachter, A. (2012) Polypyrimidine tract binding protein homologs from Arabidopsis are key regulators of alternative splicing with implications in fundamental developmental processes. Plant Cell 24, 4360–4375.
[30] Wachter, A., Ruhl, C. and Stauffer, E. (2012) The role of polypyrimidine tract-binding proteins and other hnRNP proteins in plant splicing regulation. Front. Plant Sci. 3, 81.
[31] Wang, S. and Okamoto, T. (2009) Involvement of polypyrimidine tract-binding protein (PTB)-related proteins in pollen germination in Arabidopsis. Plant Cell Physiol. 50, 179–190.
[32] Yamamoto, Y.Y., Tsuhara, Y., Gohda, K., Suzuki, K. and Matsui, M. (2003) Gene trapping of the Arabidopsis genome with a firefly luciferase reporter. Plant J. 35, 273–283.
[33] Xu, M. and Hecht, N.B. (2007) Polypyrimidine tract binding protein 2 stabilizes phosphoglycerate kinase 2 mRNA in murine male germ cells by binding to its 3′UTR. Biol. Reprod. 76, 1025–1033.
[34] Hartwig, T. et al. (2011) Brassinosteroid control of sex determination in maize. Proc. Natl. Acad. Sci. USA 108, 19814–19819.
[35] Hartwig, T., Corvalan, C., Best, N.B., Budka, J.S., Zhu, J.Y., Choe, S. and Schulz, B. (2012) Propiconazole is a specific and accessible brassinosteroid (BR) biosynthesis inhibitor for Arabidopsis and maize. PLoS One 7, e36625.
[36] Sun, L., Yu, C. and Irudayaraj, J. (2008) Raman multiplexers for alternative gene splicing. Anal. Chem. 80, 3342–3349.
[37] Sun, L., Yu, C. and Irudayaraj, J. (2007) Surface-enhanced Raman scattering based nonfluorescent probe for multiplex DNA detection. Anal. Chem. 79, 3981–3988.
[38] Cao, Y.C., Jin, R. and Mirkin, C.A. (2002) Nanoparticles with Raman spectroscopic fingerprints for DNA and RNA detection. Science 297, 1536–1540.
[39] Lamesch, P. et al. (2012) The Arabidopsis Information Resource (TAIR): improved gene annotation and new tools. Nucleic Acids Res. 40, D1202–D1210.
[40] Park, S., Sinha, N. and Hamad-Schifferli, K. (2010) Effective size and zeta potential of nanorods by Ferguson analysis. Langmuir 26, 13071–13075.
[41] Park, S. and Hamad-Schifferli, K. (2010) Enhancement of in vitro translation by gold nanoparticle∼DNA conjugates. ACS Nano 4, 2555–2560.
[42] Faulds, K., Smith, W.E., Graham, D. and Lacey, R.J. (2002) Assessment of silver and gold substrates for the detection of amphetamine sulfate by surface enhanced Raman scattering (SERS). Analyst 127, 282–286.
[43] Sun, L. and Irudayaraj, J. (2009) Quantitative surface-enhanced Raman for gene expression estimation. Biophys. J. 96, 4709–4716.
[44] Ravindranath, S.P., Kadam, U.S., Thompson, D.K. and Irudayaraj, J. (2012) Intracellularly grown gold nanoislands as SERS substrates for monitoring chromate, sulfate and nitrate localization sites in remediating bacteria biofilms by Raman chemical imaging. Anal. Chim. Acta 745, 1–9.
[45] Zimmermann, P., Hirsch-Hoffmann, M., Hennig, L. and Gruissem, W. (2004) GENEVESTIGATOR. Arabidopsis microarray database and analysis toolbox. Plant Physiol. 136, 2621–2632.
[46] Winter, D., Vinegar, B., Nahal, H., Ammar, R., Wilson, G.V. and Provart, N.J. (2007) An Electronic Fluorescent Pictograph browser for exploring and analyzing large-scale biological data sets. PLoS One 2, e718.
[47] James, A.B. et al. (2012) Alternative splicing mediates responses of the Arabidopsis circadian clock to temperature changes. Plant Cell 24, 961–981.
[48] Kriechbaumer, V., Wang, P., Hawes, C. and Abell, B.M. (2012) Alternative splicing of the auxin biosynthesis gene YUCCA4 determines its subcellular compartmentation. Plant J. 70, 292–302.
[49] Sharov, A.A., Dudekula, D.B. and Ko, M.S. (2005) Genome-wide assembly and analysis of alternative transcripts in mouse. Genome Res. 15, 748–754.
[50] Kim, E., Magen, A. and Ast, G. (2007) Different levels of alternative splicing among eukaryotes. Nucleic Acids Res. 35, 125–131.